Carbon Monoxide Dissociation on Planar and Stepped Ru(0001) Surfaces

I. M. Ciobica* and R. A. van Santen

Schuit Institute of Catalysis, Eindhoven University of Technology, P.O. Box 513, 5600 MB Eindhoven, The Netherlands

Received: January 8, 2003

The direct dissociation of CO on the Ru(0001) surface at two coverages (11.1% and 25.0%) is studied, as well as the dissociation of CO on a stepped Ru(0001) surface. Five reaction paths are studied on the planar most compact surface and four on the stepped surfaces. The indirect route for CO dissociation via the insertion of an H atom is presented for the planar surface, as well as the Boudouard reaction for the stepped surface.

1. Introduction

The adsorption of CO on metal surfaces has become the prototype system for molecular chemisorption, and a rather simple bonding model has in general been accepted. It is known that on the late transition metals the energetic difference between free and adsorbed CO (the head of adsorption) is much smaller than the C−O dissociation energy (1084 kJ mol^{-1} or 11.23 eV[1]).

The CO dissociation is important in reactions involving syn gas, such as Fischer Tropsch, where we believe that the dissociation of CO is the rate-limiting step.[2]

The CO/Ru(0001) adsorption system has been studied widely.[3,4] CO is known to adsorb nondissociatively[3] in the upright position with the C end facing the surface.[5] The adsorption is nonactivated, and a precursor model including two intrinsic and one extrinsic precursor has been proposed.[6] The adsorption energy varies with coverage from 160 to 175 kJ mol^{-1} [7,8] in the 0.33 to 0 ML coverage regime. The preferred site is the atop site for coverages up to 0.33 ML.[4]

Morikawa et al. reported DFT calculations on CO decomposition on Ni(111) and Pt(111), and the LDA results are corrected with GGA.[9] The Pt surface is found less active in dissociation, in agreement with experimental results. A late transition state presents a very long C−O bond (2.0 Å) with the C atom being adsorbed in a 3-fold site while the O atom is in a bridge site.

A database of DFT GGA calculations of the chemisorption energies of CO over hexagonal compact surfaces of Ni, Cu, Ru, Pd, Ag, Pt, Au, and Cu_3Pt is provided by Hammer et al.[10] The smallest adsorption energy is for Au(111) and Ag(111), whereas Ru(0001) gives the highest adsorption energy from this series.

In the current study, DFT calculations have been carried out to provide the geometries and the energy barriers for CO decomposition on flat and stepped Ru surfaces, via a direct or indirect route.

2. Method and Surface Model

The quantum chemical study has been performed using the VASP[11,12] code which allows periodic DFT calculations with pseudopotentials and a plane wave basis set. The approach implemented in the program is based on a generalized gradient approximation with the Perdew-Wang 91 functional.[13] The Methfessel and Paxton's smearing method[14] ($\sigma = 0.2$ eV) is applied to the electron distribution, it results that the free energy is the variational quantity and the energy is extrapolated for $\sigma = 0.0$. The interactions between the ions and the electrons are described by ultrasoft pseudopotentials (US−PP) introduced by Vanderbilt[15] and provided by Kresse and Hafner.[16]

We used a 4 layer slab with 5 vacuum layers between in a 2 × 2 supercell to describe the surface. Adsorption on both sides with an inversion center prevents the generation of dipole−dipole interactions between the supercells. The k-points sampling was generated following the Monkhorst-Pack procedure with a 5 × 5 × 1 mesh. The 3 × 3 supercell also has a 4 layer slab with 5 vacuum layers between the slabs. The k-points sampling used a 3 × 3 × 1 mesh.

To model the steps, we consider a cell with double steps, where the number of atoms in each (0001) terrace are 2 and 3, respectively. The surface can be called Ru(10$\bar{1}$5) and does not contains kink atoms.

The cutoff energy for the plane waves basis set is 400.0 eV. The coordinates of all atoms were fully optimized. All of the parameters (the k-points mesh, the number of metal and vacuum layers, etc.) were tested and carefully selected.[17]

The nudged elastic band (NEB) method developed by Jónsson et al.[18] is used to determine the transition states. This is a chain-of-states method. Two points in the hyperspace containing all of the degrees of freedom are needed (initial and final state), and a linear interpolation can be made to produce the images along the elastic band. The program will run simultaneously each image and will communicate at the end of each ionic cycle in order to compute the force acting on each image.

The term "nudged" indicates that the projection of the parallel component of true force acting on the images and the perpendicular component of the spring force are canceled. A smooth switching function is introduced that gradually turns on the perpendicular component of the spring force where the path becomes kinky at large differences in the energies between images. The images for the NEB were dynamically changed in a very similar way like in ref 19 but less automatically.

The results obtained with the NEB are refined with a quasi-Newton algorithm.[20] This implies that the atoms are moved according to minimize the forces. The total energy is not taken into account for minimization. In this way, the program is searching a stationary point. Only in the very few cases when

* To whom correspondence should be addressed. E-mail address: I.M.Ciobica@TUe.nl.

10.1021/jp030010x CCC: $25.00
Published on Web 03/29/2003

the given initial geometry is close to the geometry of the TS it is possible to reach the TS directly with the quasi-Newton technique, so the NEB is still required.

In one case, we proceeded in an alternative way. We used a cluster model to search for a TS. The geometry was ported to the periodical model, and we used the quasi-Newton algorithm to reach the saddle point.

3. Results and Discussion

In a previous paper,[21] we presented the adsorption of a CO molecule to different surfaces of Ru. Because we used NEB to calculate TSs, additional calculations were needed in order to proceed. We will first focus on the O adsorption, then on the C and O coadsorption system, and then to the TS for CO decomposition. Finally, we will discuss about the formyl group as an intermediary for CO decomposition.

3.1. C and O Adsorption. Both atomic C and atomic O strongly adsorb to the Ru(0001) surface. For the C atom, the adsorption energies and geometries were presented before[17] for the planar surface. The atomic oxygen prefers to adsorb also on hcp 3-fold hollow sites. The adsorption energies in 2×2 structures, with respect to O_2 in gas phase and bare metal surfaces, is -272 kJ mol^{-1}. It is followed by the fcc 3-fold hollow site, bridge, and atop sites with adsorption energies of -222, -207, and -122 kJ mol^{-1}, respectively. The octahedrical subsurface was investigated as well. The adsorbed oxygen is not stable; the adsorption energy is $+292$ kJ mol^{-1}. At lower coverage, in a 3×3 structure, the adsorption energy for hcp site is -266 kJ mol^{-1} showing that atomic O have a similar lateral interaction as the CH group, smaller than atomic C.

The Ru−O distances are 2.03 Å for the hcp site, 1.99 Å for the fcc site, 1.81 Å for the bridge site, and 1.77 Å for the atop site. The octahedrical subsurface sites have Ru−O bond lengths of 1.88 Å with the Ru atoms from the first layer and 2.02 Å with the Ru atoms from the second layer. All of those are for 25.0% coverage. At 11.1% coverage for the hcp site, the Ru−O distances are 2.02 Å. Atomic O's adsorbed on the edge of the steps, in a hcp site, have the following Ru−O distances: 2.01, 2.01, and 2.06 Å. Atomic C's adsorbed on the edge of the steps, in a hcp site, have the following Ru−C distances: 1.96, 1.92, and 1.92 Å.

3.2. C and O Coadsorption. Three configurations for C and O coadsorption were studied: C hcp + O hcp, C hcp + O fcc, and C fcc + O hcp. On the 2×2 structures, the adsorption energies, with respect to CO in gas phase and bare Ru surface, are -77, -47, and -17 kJ mol^{-1}, respectively. The separated adsorption of atomic C and atomic O leads to -150 kJ mol^{-1}. This shows a very large lateral repulsion between adsorbed C and adsorbed O on the Ru(0001) surface, at this coverage.

In the 3×3 structure, only the C hcp + O hcp configuration (the most stable one) was calculated. The adsorption energy is -143 kJ mol^{-1}. The separated adsorption of atomic C and atomic O leads to -183 kJ mol^{-1}. The large difference of the adsorption energies for the 2×2 and 3×3 is caused by the important lateral interactions between atomic carbons[22] and between atomic oxygens.

For the coadsorption on the Ru steps, we consider four cases: both C and O adsorbed up the step, both adsorbed down the step, and one up, one down, in all of the cases only the hcp sites (the most stable). The adsorption energies are -110 kJ mol^{-1} for C hcp up + O hcp up, -99 kJ mol^{-1} for C hcp up + O hcp down, -24 kJ mol^{-1} for C hcp down + O hcp down, and -121 kJ mol^{-1} for C hcp down + O hcp up. The separated adsorption of atomic C and atomic O on steps leads to an adsorption energy of -163 kJ mol^{-1}. Again, this shows a very large lateral repulsion between adsorbed atomic C and adsorbed atomic O.

The geometries of coadsorbed atomic C and atomic O follows. In the 2×2 structures, the Ru−C bond lengths are between 1.91 and 1.97 Å, and Ru−O bond lengths are between 2.01 and 2.04 Å. In the 3×3 structure, the Ru−C bond lengths are 1.91, 1.94, and 1.96 Å, whereas the Ru−O bond lengths are 1.99, 2.02, and 2.07 Å. For the coadsorption on stepped surface, the Ru−C bond lengths are between 1.92 and 1.98 Å, similar with those of the bare surface. The Ru−O bond lengths are between 2.01 and 2.06 Å. In general, the geometries of atomic C and atomic O coadsorption do not differ significantly from the separated adsorption.

3.3. CO Decomposition. Adsorbed CO has been discussed elsewhere.[21] We will focus here only on the transition states for CO decomposition. The TSs considered are

1. (2×2) CO hcp → C hcp + O hcp
2. (2×2) CO atop → C hcp + O hcp
3. (2×2) CO hcp → C hcp + O fcc
4. (2×2) CO fcc → C fcc + O hcp
5. (3×3) CO hcp → C hcp + O hcp
6. (steps) CO hcp up → C hcp up + O hcp up
7. (steps) CO hcp down → C hcp down + O hcp down
8. (steps) CO hcp down → C hcp down + O hcp up
9. (steps) CO hcp up → C hcp up + O hcp down

The TS1 is sometimes called the TS "over the valley", to be distinguish from TS3, which is "over the top". In TS1, the CO molecule is tilting and the O atom arrives in an asymmetric bridge position. The C atom is assisting the move of the O atom. The barrier for TS1 is 227 kJ mol^{-1}, see Figure 1.

Because atop is the preferred adsorption site for CO, we investigated the possibility of a dissociative path starting with CO atop, TS2. The results of the NEB path show that in fact the CO is migrating in a nearby hcp site before the actual dissociation starts. If we constrain the system to start the dissociation before the CO will move on the hcp site, then the barrier is about 329 kJ mol^{-1}.

TS3 is not the favorite dissociation mechanism. The calculations show a barrier of 238 kJ mol^{-1}. This is due to the fact that the O atom will not be favorably adsorbed on the fcc site on Ru(0001) surface.

Starting the dissociation with CO in a fcc site, with a mechanism over the top, TS4, will produce an atomic O in a hcp site, more stable than the fcc site. However, this puts the initial CO and the final C in a fcc site which are less stable. This TS shows a high barrier of 318 kJ mol^{-1}.

We have shown before that TS1 is the preferred path for CO dissociation. TS5 is in fact TS1, but at lower coverage, 11.1% instead of 25.0%. The barrier is 216 kJ mol^{-1}, 11 kJ mol^{-1}less than that in 2×2 structure, see Figure 2.

For stepped surfaces, TS6 and TS7 are TS1-like, but along the edge or the bottom of the step. The barriers are similar, and the influence of the step is not important in those cases.

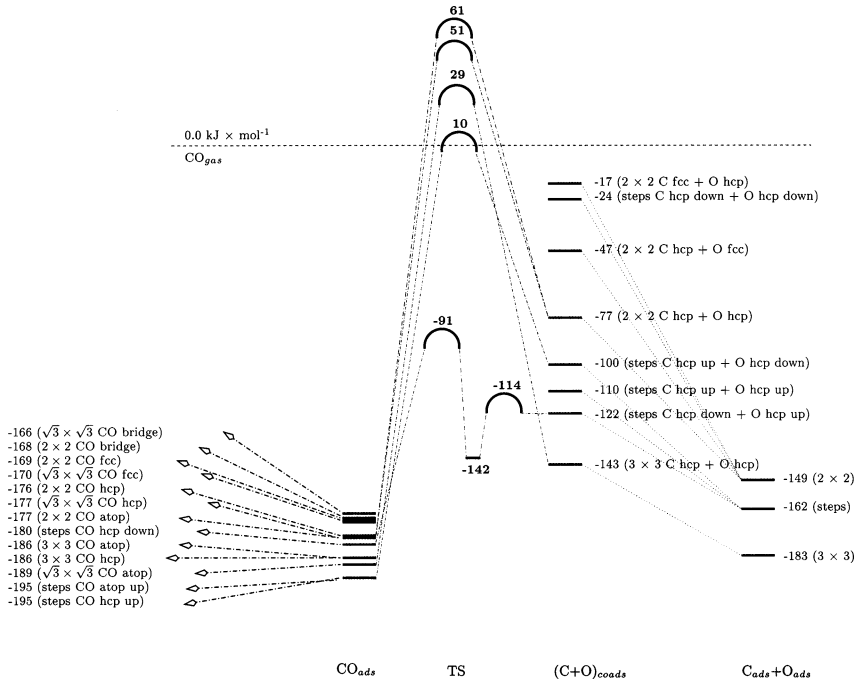

Figure 1. CO direct decomposition path. At left are levels for CO adsorption, and at right are the levels for C and O coadsorption, sharing or not a metal atom on the surface. TS3 and TS4 are not shown; they are much higher.

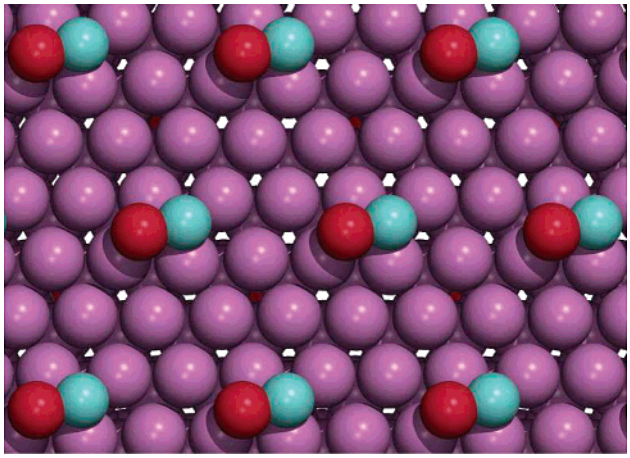

Figure 2. TS for CO decomposition on flat Ru(0001) surface.

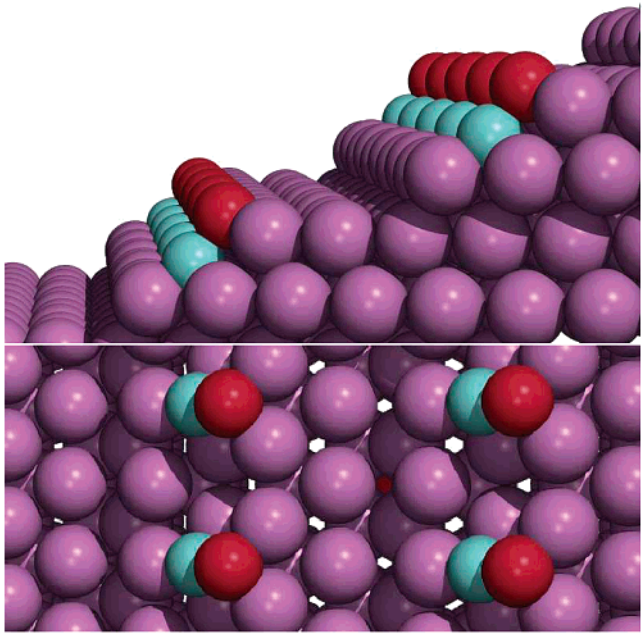

Figure 3. TS for CO decomposition on stepped Ru(0001) surface, side and top view.

TS8 is found when CO is adsorbed at the bottom of the step, and the dissociation occurs with the O atom going up, over the step. This reaction path is very interesting. Just after the TS, a small minimum is when the O atom is in a bridge site formed by two metal atoms at the edge. This adsorption site is more stable than a normal bridge site because of the lower coordination number of the metal atoms at the step. The first TS is an early one. Soon after the reaction starts, the C and O are not any longer in contact, and they even do not share a metal atom like it would be the case on the terrace. The barrier is 89 kJ mol^{-1}, see Figure 3. The second barrier is less important and it is of the same order of magnitude as for the barriers for CO diffusion.

TS9 is found for CO adsorbed at the edge of the step with dissociation of the O atom going down, over the step. This reaction path is less probable because there are less possibilities that the O atom is stabilized in the TS. The barrier is 205 kJ mol^{-1}, 126 kJ mol^{-1} more than TS8.

The geometry of TS5 and TS8 follows. The C−Ru bond lengths are 1.99, 1.98, and 1.94 Å for TS5 and 1.99, 1.99, and 1.94 Å for TS8. On the flat surface, the C atom is assisting the O atom in it's movement. The O−Ru bond lengths are 2.09 and 2.06 Å for TS5 and 2.00 and 2.00 Å for TS8. The C−O distances are 1.84 and 1.97 Å for TS5 and TS8, respectively. The geometry of TS1 is in within 0.02−0.04 Å like TS5.

3.4. CO Disproportionation. We also studied the Boudouard reaction (disproportionation of CO): $2\ CO_{ads} \rightarrow C_{ads} + CO_2$, only on steps. One CO molecule is adsorbed at the bottom of the step, and the other one is adsorbed at the edge of the step. The O atom from the CO molecule sitting at the bottom of the step is moving toward the step; the same way it would do it for CO dissociation in TS8. At some point, interactions with the other CO molecule start to form and an adsorbed nonlinear CO_2 (indicative of negative charged species) will form, which can desorb. The reaction barrier is 152 kJ mol^{-1} with respect to

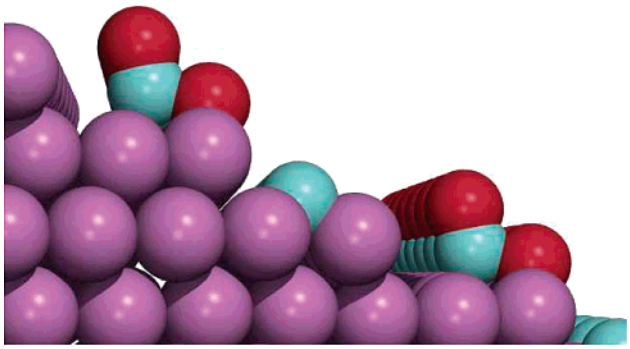

Figure 4. TS for CO disproportionation on stepped Ru(0001) surface.

two adsorbed CO molecules. This TS was not calculated with NEB, see before (model).

The geometry of the TS for the Boudouard reaction follows. The C atom which remained at the bottom of the step has two Ru−C bond lengths of 1.97 Å, and one bond length of 1.88 Å. The other C atom has longer distances: 2.03, 2.82, and 2.84 Å to the metal atoms. The C−O bond lengths are 1.18 and 1.77 Å. The O−Ru bond lengths are 2.05 and 2.02 Å, for the O atom which is claiming the step edge. The O−C−O angle is 114°, see Figure 4.

3.5. CO Decomposition via H Insertion. To understand CO decomposition, specially in a mixture with H_2 (syn gas), we investigated the possibility of an insertion of a hydrogen atom to the adsorbed CO molecule, followed by the C−O dissociation.

The CHO radical is found to be adsorbed on a hcp site. The adsorption energy is −124 kJ mol^{-1} with respect to CO and H_2 gas phase and Ru bare surface. This radical is not very stable; the adsorption energy of CH hcp and O hcp sharing one Ru atom is −190 kJ mol^{-1}, whereas the adsorption energy of CO hcp and H fcc sharing one Ru atom is −230 kJ mol^{-1}.

In Figure 5, we can see the reaction path of a CO molecule dissociating via a hydrogen insertion. The TS for the CHO formation is extremely low, just 37 kJ mol^{-1} above its energy of formation, for the reaction path of CO top + H fcc, whereas in the cases when CO is adsorbed on hcp sites (and the H atom either of fcc or hcp sites), the barrier is within the error limits. CHO shows a similar stability on Pd(111).[23] However, there the barrier for H addition to CO is with 18 kJ mol^{-1} above the energy of formation of the formyl species. On Ru(0001) the TS for the CHO decomposition is also small, 30 kJ mol^{-1} with respect to adsorbed CHO. The CH and O formed have to diffuse away from each other, and then the CH has to dissociate to form atomic C and atomic H. The overall barrier for the CO dissociation via this mechanism is 143 kJ mol^{-1}, which is smaller than the one involved via TS1. On steps, we expect those barriers to be similar. Furthermore, even if the barriers drop out, still the reaction enthalpy over 100 kJ mol^{-1} is higher than the barrier for CO decomposition over the steps with mechanism TS8.

4. Conclusion

CO dissociation on transitional metal surfaces is an important topic to catalysis. Ruthenium is a metal which is at the borderline of metals which easily dissociate or do not easily dissociate the CO. Our calculations show that the preferred reaction path for dissociation is over the valley formed by the neighboring atoms. The TS energy has a coverage dependency. The difference between the barrier on 2 × 2 (25.0% coverage) and 3 × 3 (11.1 coverage) is 11 kJ mol^{-1}.

On steps the lowest reaction path for CO dissociation proceeds through adsorption of CO at the bottom of the step and the O atom jumping on the next terrace. The barrier for this reaction is only 89 kJ mol^{-1}.

The Boudouard reaction is leasest probable to occur. The barrier on the steps is higher than for CO dissociation with 63 kJ mol^{-1}. We expect that on the planar surface this difference is higher.

CHO as intermediate for CO decomposition has also been investigated. This indirect route for CO dissociation, which is favorable on Pd, is not preferred on Ru. The overall barrier for the indirect path on flat surface is indeed smaller than the direct dissociation path on flat surface, but over the steps, the barrier for direct dissociation is smaller than the reaction enthalpy for the indirect route.

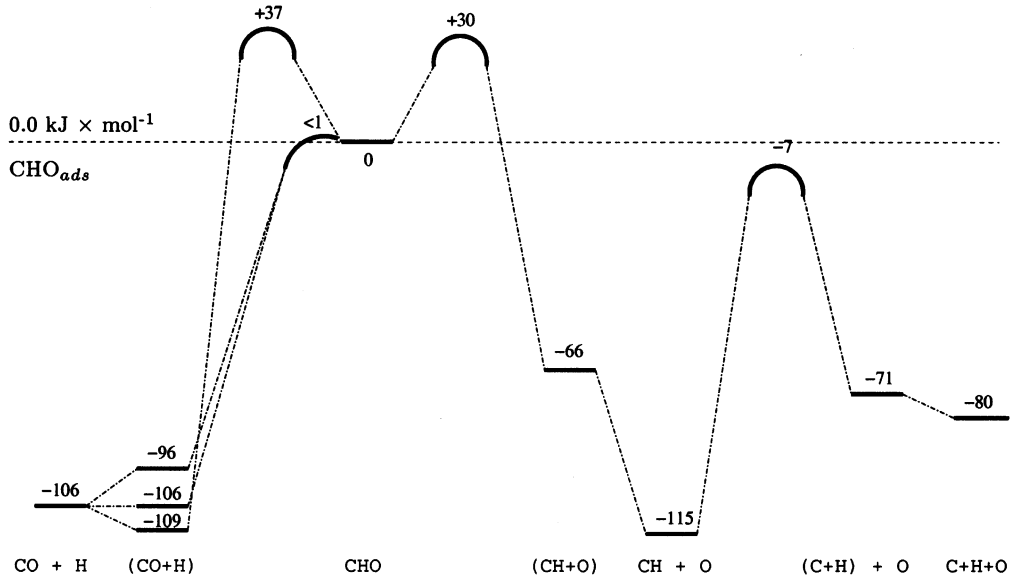

Figure 5. CO decomposition path via H insertion. At left is CHO formation from CO and H, and at right is CHO decomposition to CH and O, followed by CH decomposition. The three levels from (CH+O) are from down upward: CO top + H fcc, CO hcp + H fcc, and CO hcp + H hcp.

Acknowledgment. This work is part of the research program of the "Stichting voor Fundamenteel Onderzoek der Materie (FOM)", which is financially supported by the "Nederlandse organisatie voor Wetenschappelijk Onderzoek (NWO)". This work has been accomplished under the auspices of NIOK, The Netherlands Institute for Catalysis Research, Lab Report No. TUE-2001-5-5. The calculation have been partially performed with NCF support (SC183, MP43b). The authors thank Prof. Dr. Hafner for the vasp code.

References and Notes

(1) Toyoshima, I.; Somorjai, G. A. *Catal. Rev. Sci. Eng.* **1997**, *19*, 105.
(2) Ciobica, I. M.; Kramer, G. J.; Ge, Q.; Neurock, M.; van Santen, R. A. *J. Catal.* **2002**, *212*, 136.
(3) Fuggle, J. C.; Madey, T. E.; Steinkilberg, M.; Menzel, D. *Surf. Sci.* **1975**, *52*, 521.
(4) Pfnür, H.; Menzel, D.; Hoffmann, F. M.; Ortega, A.; Bradshaw, A. M. *Surf. Sci.* **1980**, *93*, 431.
(5) Fuggle, J. C.; Madey, T. E.; Steinkilberg, M.; Menzel, D. *Chem. Phys.* **1975**, *11*, 307.
(6) Pfnür, H.; Menzel, D. *J. Chem. Phys.* **1983**, *79*, 2400.
(7) Pfnür, H.; Feulner, P.; Menzel, D. *Chem. Phys. Lett.* **1979**, *59*, 481.
(8) Pfnür, H.; Feulner, P.; Menzel, D. *J. Chem. Phys.* **1983**, *79*, 4613.
(9) Morikawa, Y.; Mortensen, J. J.; Hammer, B.; Nørskov, J. K. *Surf. Sci.* **1997** *386*, 67.
(10) Hammer, B.; Morikawa, Y.; Nørskov, J. K. *Phys. Rev. Lett.* **1996**, *76*, 2141.
(11) Kresse, G.; Furthmüller, J. *Comput. Mater. Sci.* **1996**, *6*, 15.
(12) Kresse, G.; Furthmüller, J. *Phys. Rev. B* **1996**, *54*, 169.
(13) Perdew, J. P. *Electronic Structure of Solids '91*; Akademie Verlag: Berlin, 1991.
(14) Methfessel, M.; Paxton, A. T. *Phys. Rev. B* **1989**, *40*, 3616.
(15) Vanderbilt, D. *Phys. Rev. B* **1990**, *41*, 7892.
(16) Kresse, G.; Hafner, J. *J. Phys.: Condens. Matter* **1994**, *6*, 8245.
(17) Ciobica, I. M.; Frechard, F.; van Santen, R. A.; Kleyn, A. W.; Hafner, J. *Chem. Phys. Lett.* **1999**, *311*, 185.
(18) Jónsson, H.; Mills, G.; Jacobsen, K. W. In *Classical and Quantum Dynamics in Condensed Phase Simulations*; Berne, B. J., Ciccotti, G., Coker, D. F., Eds.; 1998.
(19) Maragakis, P.; et al. *J. Chem. Phys.* **2002**, *117* 10, 4651.
(20) Pulay, P. *Chem. Phys. Lett.* **1980**, *73*, 393.
(21) Ciobica, I. M.; Kleyn, A. W.; van Santen, R. A. *J. Chem. Phys. B* in press.
(22) Ciobica, I. M.; Frechard, F.; Jansen, A. P. J.; van Santen, R. A. *Stud. Surf. Sci.* **2001**, *133*, 221.
(23) Neurock, M. *Top. Catal.* **1999**, *9*, 135.